The Astrophysical Journal, 476:766–770, 1997 February 20

VOYAGER MEASUREMENTS OF THE MASS COMPOSITION OF COSMIC-RAY Ne, Mg, Si, AND S NUCLEI

W. R. Webber,[1] A. Lukasiak,[2] and F. B. McDonald[2]
Received 1996 July 1; accepted 1996 September 6

ABSTRACT

We report new measurements of the mass composition of cosmic-ray Ne, Mg, Si, and S nuclei made on the *Voyager* spacecraft. These measurements have $\sim$4 times the statistical accuracy of previously published measurements covering these four charges. With the new cosmic-ray source mass fractions of these elements that we obtain, only the isotope ^{22}Ne shows a cosmic-ray source abundance that is significantly different from the solar abundances. The limits of $\pm 15\%$ that we set on the cosmic-ray source-to-solar abundance ratios of ^{25}Mg/^{24}Mg and ^{26}Mg/^{24}Mg as well as the heavier Si isotopes place severe limits on the models that have been proposed to explain compositional differences between galactic cosmic rays and solar system abundances. The only two statistically significant isotopic differences between the cosmic-ray source and the solar system in the charge range $Z = 6$–16 now appear to be the underabundance of ^{14}N and the overabundance of ^{22}Ne. This suggests to us that the helium-burning process in which ^{14}N is turned into ^{22}Ne plays an important role in at least some of the sources of those particles ultimately accelerated as cosmic rays.

Subject headings: cosmic rays — nuclear reaction, nucleosynthesis, abundances — space vehicles

1. INTRODUCTION

The mass composition of cosmic rays at their source has certain distinctive differences with solar system abundances. The most clearly established differences involve the overabundance of ^{22}Ne and the underabundance of ^{14}N in the cosmic-ray sources relative to solar abundances, for example. These differences have been used to try to understand possible differences in the nucleosynthetic history of the cosmic-ray sources and solar system material and have led to suggestions that Wolf-Rayet stars may be the source of some of the cosmic rays (Casse & Paul 1982) or that the sources of cosmic rays may have a high metallicity leading to an overabundance of neutron-rich isotopes (Woosley & Weaver 1981). Each model has its own specific predictions for the enhancement of neutron-rich isotopes, and the observation by the first truly high mass resolution instrument on *ISEE 3* that the isotopes ^{25}Mg, ^{26}Mg, ^{29}Si, and ^{30}Si in addition to ^{22}Ne appeared to be enhanced in the cosmic-ray sources relative to the solar mass fractions (Wiedenbeck & Greiner 1981) gave those ideas a big boost. Subsequently, it was shown that much of this excess of heavier isotopes for both Mg and Si could be explained away by the use of new cross sections that resulted in the increased production of these isotopes in interstellar interactions (Webber et al. 1990d).

In recent years, a new generation of high-resolution spacecraft experiments (Lukasiak et al. 1993; Connell & Simpson 1993) have obtained source abundances of the Mg and Si isotopes that are much more closely solar. But these new measurements have been limited mainly by the statistical accuracy of the measurements themselves as to how well the source abundances of all the Ne, Mg, Si, and S isotopes match those determined for the Sun.

In this paper, we report new measurements of the isotopic composition of these elements using cosmic-ray telescopes on the *Voyager* spacecraft. These measurements, which are an extension of those reported earlier by Lukasiak et al. (1994), increase the statistics of the earlier measurements by a factor $\sim$4 as a result of the long duration of the *Voyager* mission, while at the same time maintaining acceptable mass resolution.

2. OBSERVATIONS AND DATA ANALYSIS

The data from the High Energy Telescope (HET) of the CRS experiment on both the *Voyager 1* and *2* spacecraft from 1977 to 1996 have been used in this analysis. This telescope (Fig. 1) has been described extensively previously (Stone et al. 1977), and the charge and mass analysis of the telescope events follow closely that described by Lukasiak et al. (1994). The first step in the analysis of the experimental data is the removal of background events, which is accomplished by using two independent dE/dx versus E (energy) analyses to reject events that are not consistent. Using an energy loss program, we calculated the theoretical tracks in dE/dx versus E space for each charge. These tracks are fitted to the data for the elements $Z = 10$–16 in this analysis. For every event, we have determined a charge value from the position of the event with respect to the closest charge track as described by Ferrando et al. (1991). In Figure 2 we show a scatter plot of charge consistency versus charge for the selected events with $Z = 10$–16. The overall charge resolution for these elements is $\sim$0.07 charge units.

In the next stage of data analysis, we determined for each event two mass values, A_1 and A_2, corresponding to the analysis of B_1 versus ΣC and B_2 versus ΣC pulse height data where $\Sigma C = C_2 + C_3 + C_4$. For every element, we generated theoretical simulated mass lines corresponding to the different isotopes. A mass value was then determined for every event from the position of the event with respect to the closest mass track. The simulation tracks were then further adjusted slightly to fit the distribution of events corresponding to different isotopes and to optimize the mass resolution for the key isotopes of each charge ^{20}Ne, ^{24}Mg, ^{28}Si, and ^{32}S. The HET telescope has three dead layers of

[1] Astronomy Department, New Mexico State University, Las Cruces, NM.

[2] Institute for Physical Science and Technology, University of Maryland, College Park, MD.

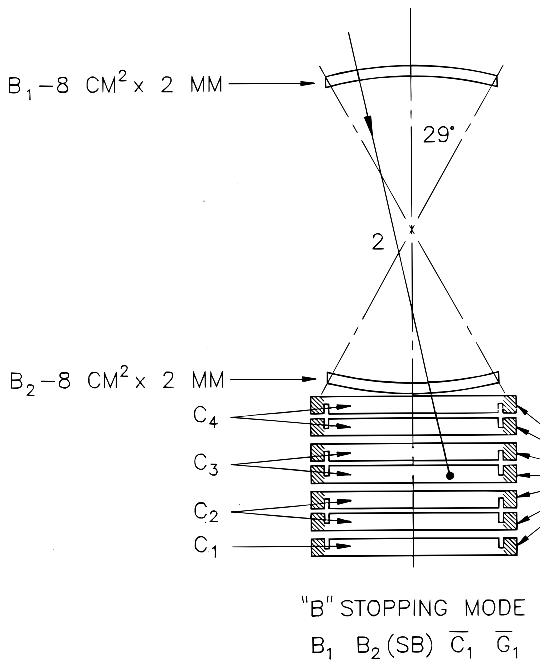

FIG. 1.—Outline drawing of the HET telescope of the *Voyager* detector system.

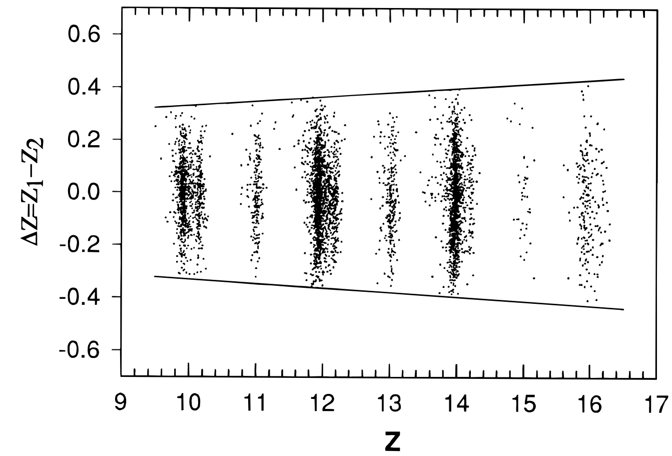

FIG. 2.—Scatter plot of charge consistency vs. charge for $Z = 10$–16 nuclei events within the 3 σ (*solid lines*) consistency criterion.

material between the individual C counters, and events stopping in the dead layers have mass values that are not as well resolved. To improve the mass resolution, we removed all events stopping in the dead layers. This decreased the number of events by $\sim$20%.

Figure 3 shows the mass histograms for the elements Ne, Mg, Si, and S in the combined *Voyager 1* and *2* spacecraft measurements from 1977 to 1996. The solid lines in Figure 3 correspond to a fit of a multi-Gaussian function to the isotope distributions. These isotope functions are spaced at fixed 1.0 amu intervals and have individual resolutions of 0.26, 0.31, 0.37, and 0.42 amu for each Ne, Mg, Si, and S element, respectively.

The event breakdown and isotopic ratios are given in Table 1. In these calculations the isotope ratios were corrected for the slightly different energy intervals for each isotope, resulting in differences in the widths of the energy intervals and also differences because of the spectra of the particles, assumed here to have a spectral index $= -0.80$. A 5% correction was also made to the abundance of ^{20}Ne for the presence of anomalous ^{20}Ne at the lowest energies. These effects introduced changes of less than 10% in any of the isotopic ratios for a given charge.

The errors on the measured isotope ratios are dominated in most cases by the statistical errors on the number of events and include fitting errors (important for ^{29}Si and ^{33}S) and the errors resulting from the adjustments to common energy intervals.

The results of this study of 18 years correspond to an average level of solar modulation $\phi = 480$ MV with a range

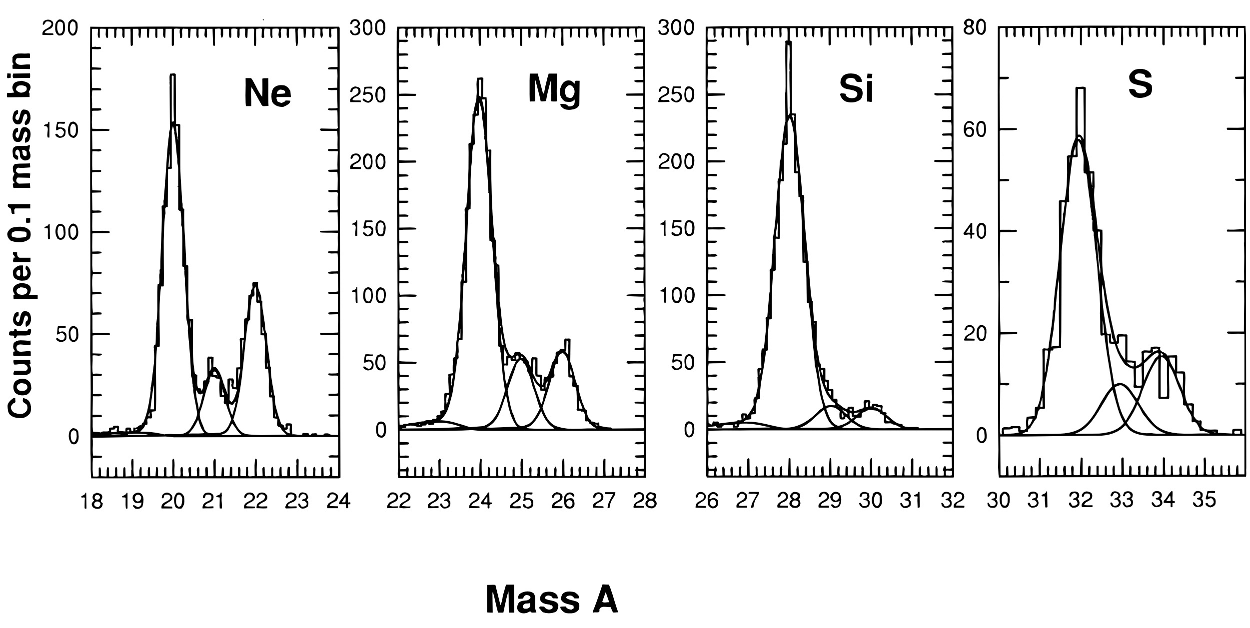

FIG. 3.—Mass histograms for the elements Ne, Mg, Si, and S showing fitted Gaussian functions

TABLE 1

ISOTOPIC COMPOSITION OF Ne, Mg, Si, AND S NUCLEI
(*Voyager 1* AND *2*, 1977–1996, $\phi = 480$ MV)

Isotopic Ratio	Number of Events	Energy Range (MeV nucleon^{-1})	Measured Isotopic Ratio
^{20}Ne/Ne	1046, 1766	65–150	0.571 ± 0.012
^{21}Ne/Ne	214, 1766	65–150	0.126 ± 0.009
^{22}Ne/Ne	506, 1766	65–150	0.304 ± 0.012
^{21}Ne/^{20}Ne	214, 1046	66–153	0.221 ± 0.019
^{22}Ne/^{20}Ne	506, 1046	66–153	0.533 ± 0.029
^{24}Mg/Mg	2032, 2948	73–169	0.675 ± 0.0096
^{25}Mg/Mg	435, 2948	73–169	0.151 ± 0.0086
^{26}Mg/Mg	481, 2948	73–169	0.174 ± 0.0079
^{25}Mg/^{24}Mg...	435, 2032	74–170	0.223 ± 0.013
^{26}Mg/^{24}Mg...	481, 2032	74–170	0.257 ± 0.015
^{28}Si/Si.........	2219, 2522	80–186	0.8742 ± 0.0087
^{29}Si/Si.........	161, 2522	80–186	0.0657 ± 0.0085
^{30}Si/Si.........	142, 2522	80–186	0.0600 ± 0.0055
^{29}Si/^{28}Si	161, 2219	80–187	0.078 ± 0.010
^{30}Si/^{28}Si	142, 2219	80–187	0.069 ± 0.006
^{32}S/S	332, 469	86–230	0.69 ± 0.03
^{33}S/S	59, 469	86–230	0.128 ± 0.028
^{34}S/S	78, 469	86–230	0.180 ± 0.024

of $\sim$250–1000 MV at the *Voyager* spacecraft. These modulation levels were estimated on a yearly basis using the He spectrum measured at *Voyager 1* and *Voyager 2* for that year and the modulation model described by Ferrando et al. (1991). The resulting values of ϕ for each year are shown in Figure 4. The overall average modulation for this measurement is about equivalent to the modulation observed near the Earth at sunspot minimum.

3. INTERPRETATION OF RESULTS

The interpretation of these experimental results requires a model for the propagation of cosmic rays in the galaxy. As a point of reference for earlier calculations, we performed these calculations using a standard leaky-box model with a simple exponential distribution of path lengths through the interstellar material. The most essential components of this model are (1) the source composition, (2) the source spectral

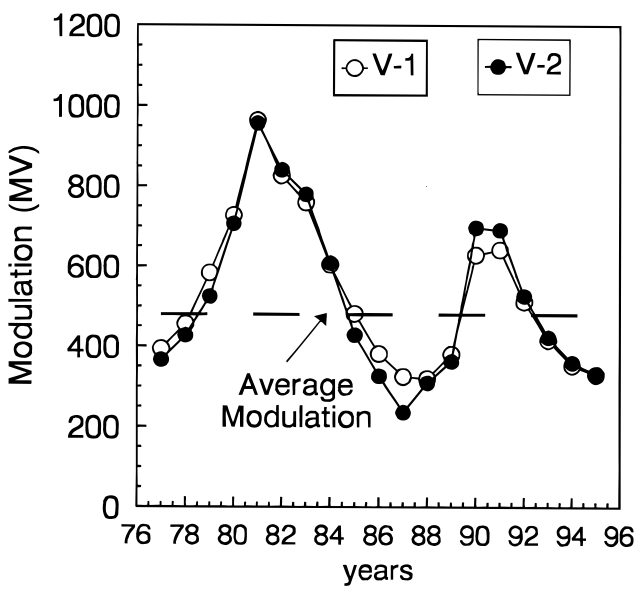

FIG. 4.—Yearly average solar modulation values obtained from He spectra measured on *Voyager 1* and *Voyager 2*.

shape, (3) the composition of the interstellar medium (ISM), (4) the fragmentation cross sections, (5) the interstellar path lengths as a function of energy, and (6) the effects of solar modulation.

For the source composition, we took the abundances used previously by Lukasiak et al. (1994), which are essentially solar system abundances except for ^{22}Ne. The source spectral shape was taken to be a power law in rigidity with an index of -2.36. We assumed that the ISM is 90% hydrogen and 10% helium by number with an ionized fraction of 30% as described by Soutoul, Ferrando, & Webber (1990). This increases the energy loss by ionization over that of a neutral medium. For the interstellar fragmentation, we used the measured and parametric cross sections in hydrogen given by Webber, Kish, & Schrier (1990a, 1990b, and 1990c) and the helium cross sections from Ferrando et al. (1988).

We have considered two possibilities for the interstellar path length; $\lambda_{esc} = 31.6\beta R^{-0.60}$ for rigidities $R > 4.7$ GV ($= 12.5\beta$ g cm^{-2} for $R < 4.7$ GV), which provides a best fit to the B/C ratio (Webber et al. 1996), and $\lambda_{esc} = 40.6\beta R^{-0.70}$ for rigidities $R > 3.3$ GV ($= 17.1\beta$ g cm^{-2} for $R < 3.3$ GV), which provides a best fit to the ($Z = 21$–23)/Fe ratio (Lukasiak et al. 1995). These different values for λ_{esc} may imply that the path length distribution is not strictly an exponential and are used here to set limits on possible uncertainties arising from interstellar propagation. For solar modulation effects, we have considered values of ϕ ranging from 400 to 600 MV in order to determine the uncertainty in the calculations as a result of uncertainties in solar modulation effects.

A comparison between our new results on Ne, Mg, Si, and S and the propagation calculations is shown in Table 2. Note that the differences between the measured ratios and calculated secondary ratios gives directly the mass ratios at the source. Previous results from other experiments on these elements have been described in Lukasiak et al. (1994) and will not be repeated here except to note that these new results agree closely with the high mass resolution *Ulysses* results (Connell & Simpson 1993). We wish to point out, however, that the statistics of the new results are a factor of $\sim$4 better than any of the earlier results. The assignment of measurement errors for our new results has already been discussed. For the errors on the secondary contribution, which includes both galactic propagation and solar modulation uncertainties, we have assumed that the overall error due to cross secton uncertainties is ± 5% for the measured cross sections and ± 15% for those obtained from the formula as per our earlier calculation (Lukasiak et al. 1994). For the uncertainty in the interstellar path length, we took the average of the results of the two path length calculations described above with the two extremes providing the fractional error. And finally for the modulation we took an uncertainty of ± 50 MV. The total error for the secondary calculation was then obtained by adding the above errors in quadrature (see below for an alternate estimate of the propagational errors using the tracer technique with ^{21}Ne).

We will now discuss the source abundances obtained as a function of charge.

Neon.—The isotope ^{21}Ne is interesting as a tracer of interstellar production and solar modulation effects, as well as uncertainties in these effects (just like the B/C ratio) because of the expected low source abundance and the large secondary production of this isotope (Stone & Wiedenbeck

TABLE 2

ISOTOPIC COMPOSITION OF Ne, Mg, Si, AND S NUCLEI AT THE COSMIC-RAY SOURCE
(*Voyager 1* AND *2*, 1977–1996, $\phi = 480$ MV)

Isotopic Ratio	$\bar{E}$ (MeV nucleon^{-1})	Measured Ratio	Secondary Contribution	Fraction at Source	Ratio CRS/Solar
^{21}Ne/^{20}Ne	122	0.222 ± 0.018	0.207 ± 0.015	...	...
^{22}Ne/^{20}Ne	122	0.533 ± 0.029	0.194 ± 0.014	0.337 ± 0.032	2.78 ± 0.25(NeA)
					4.72 ± 0.43(SW)
^{25}Mg/^{24}Mg......	131	0.223 ± 0.013	0.087 ± 0.006	0.136 ± 0.015	1.06 ± 0.12
^{26}Mg/^{24}Mg......	131	0.257 ± 0.013	0.086 ± 0.006	0.164 ± 0.015	1.15 ± 0.11
^{29}Si/^{28}Si	144	0.078 ± 0.009	0.037 ± 0.003	0.041 ± 0.009	0.80 ± 0.18
^{30}Si/^{28}Si	144	0.069 ± 0.006	0.034 ± 0.003	0.035 ± 0.006	1.03 ± 0.16
^{33}S/^{32}S...........	172	0.186 ± 0.038	0.200 ± 0.018	...	...
^{34}S/^{32}S...........	172	0.262 ± 0.031	0.214 ± 0.018	0.048 ± 0.033	1.07 ± 0.67

1979). The tracer approach permits a quantitative evaluation of the total effect of propagational and observational uncertainties on the deduced source abundance. The agreement between the measured ^{21}Ne/^{20}Ne ratio of 0.221 ± 0.018 and the predicted secondary ratio of 0.207 means that the magnitude of any systematic uncertainties in either propagational or modulation effects for all isotopes considered here must indeed be known to $\sim \pm 7\%$ or less, the difference in the measured and predicted ^{21}Ne/^{20}Ne ratio. This is slightly less than the quadratic sum of the formal uncertainties discussed earlier, but for the purpose of the total errors (e.g., in Table 2) we use the formal error analysis.

For the ^{22}Ne/^{20}Ne source fraction, we obtain $33.7\% \pm 3.1\%$, or 2.78 times the standard solar abundance fraction if meteoritic abundances are used (neon-A) (e.g., Cameron 1982). If the solar wind ratio of 0.073 for these isotopes is used as a standard (e.g., Anders & Ebihara 1982), the enhancement is a factor of 4.7.

Magnesium.—The ^{25}Mg/^{24}Mg and ^{26}Mg/^{24}Mg source fractions that we derive are 0.136 ± 0.015 and 0.164 ± 0.015, respectively. These fractions are 1.06 ± 0.12 and 1.15 ± 0.11 times the solar mass fractions. These isotopes show no enhancement over the solar abundances to a level of $\pm 15\%$.

Silicon.—The ^{29}Si/^{28}Si and ^{30}Si/^{28}Si source fractions that we derive are 0.041 ± 0.009 and 0.035 ± 0.005, respectively. These fractions are 0.80 ± 0.18 and 1.03 ± 0.16 times the solar mass fractions of 0.051 and 0.034. These isotopes are also consistent with solar abundances to a level of $\pm 15\%$.

Sulphur.—As in the case of ^{21}Ne, the source abundance of ^{33}S is dominated totally by the secondary production. So it serves as a tracer, albeit with much less sensitivity than the *B* and ^{21}Ne tracers. The ratio of the measured to calculated secondary ^{33}S/^{32}S ratio is 0.93 ± 0.19.

For the ^{34}S/^{32}S cosmic-ray source ratio, we obtain 0.048 ± 0.033 as compared with the solar ratio of 0.045. The accuracy of this comparison is dominated by the ^{34}S statistics, but this ratio is not inconsistent with the solar abundance ratio.

4. SUMMARY AND CONCLUSIONS

Only the isotope ^{22}Ne among the six isotopes that are referenced here has a source abundance that is clearly not solar. The lack of enhancement of ^{25}Mg or ^{26}Mg at the 15% level is particularly important and places stringent limits on both the Wolf-Rayet contribution to the cosmic-ray sources as described originally by Casse & Paul (1982) or a supermetallicity model as described by Woosley & Weaver (1981). In Wolf-Rayet–type stars, an excess of ^{22}Ne is certainly expected as a result of helium burning; however, it is not clear just how much of this ^{22}Ne is expelled by the strong stellar winds and eventually is accelerated as cosmic rays (Prantzos et al. 1986). If the cosmic-ray source excess is adjusted to fit the measured ^{22}Ne excess, then the original model of Casse & Paul predicts an excess of both ^{25}Mg and ^{26}Mg at the source by a factor of ~ 1.5. Our new measurements are certainly inconsistent with such a large enhancement.

The supermetallicity model as presented by Woosley & Weaver predicts an enhancement by a factor of ~ 1.5–2 for all the heavier isotope ratios ^{18}O/^{16}O, ^{22}Ne/^{20}Ne, the two Mg, and the two Si isotope ratios. Again, outside of ^{22}Ne/^{20}Ne, which is actually enhanced much more than this, none of these ratios show the expected enhancement, including the ^{18}O/^{16}O ratio obtained from our recent *Voyager* measurement (Webber et al. 1996).

So, in effect, none of the above modifications to the standard nucleosynthesis picture of the solar composition seem to do an acceptable job of explaining the observed differences between the cosmic-ray source and the solar abundances in the charge range $Z = 6$–16. These differences appear to be less extensive than thought previously, and as we have noted, they center on a few rather well-defined differences. Excluding possible first ionization potential related charge differences, these differences include (1) the excess ^{22}Ne abundance, (2) the much lower ^{14}N abundance, and (3) the possible low abundance of ^{13}C as discussed in Lukasiak et al. (1994) and Webber et al. (1996).

If, out of all the many possibilities for galactic cosmic-ray and solar composition differences in this charge range, these three (or two) are the only significant isotopic differences observed, this would seem to point to a particular feature of the nucleosynthesis process. Such a connection may indeed be the helium-burning process in which the ^{14}N, produced in the initial H burning, is turned into ^{22}Ne. This process immediately suggests an explanation for both the underabundance of ^{14}N and the overabundance of ^{22}Ne. Exactly how this reaction operates in a way to be reflected in the source composition of the accelerated cosmic rays still needs to be explained fully.

The authors wish to thank the *Voyager* project office at JPL for its support through contract No. 959213 at the University of Maryland and contract No. 959160 at New Mexico State University.

REFERENCES

Anders, E., & Ebihara, M. 1982, Geochim. Cosmochim. Acta, 4b, 2363
Cameron, A. G. W. 1982, in Essays in Nuclear Astrophysics, ed. C. A. Barnes, D. D. Clayton, & D. N. Schramm (Cambridge: Cambridge Univ. Press), 23
Casse, M., & Paul, J. A. 1982, ApJ, 258, 860
Connell, J. J., & Simpson, J. A. 1993, Proc. 23rd Int. Cosmic-Ray Conf. (Calgary), 1, 559
Ferrando, P., Lal, N., McDonald, F. B., & Webber, W. R. 1991, A&A, 247, 163
Ferrando, P., et al. 1988, Phys. Rev. C, 37, 1490
Lukasiak, A., Ferrando, P., McDonald, F. B., & Webber, W. R. 1993, Proc. 23rd Int. Cosmic-Ray Conf. (Calgary), 1, 539
———. 1994, ApJ, 426, 366
Lukasiak, A., McDonald, F. B., Webber, W. R., & Ferrando, P. 1995, Proc. 24th Int. Cosmic-Ray Conf. (Rome), 2, 576
Prantzos, N., Doom, C., Arnould, M., & de Loore, C. 1986, ApJ, 304, 695
Soutoul, A., Ferrando, P., & Webber, W. R. 1990, Proc. 21st Int. Cosmic-Ray Conf. (Adelaide), 3, 337
Stone, E. C., & Wiedenbeck, M. E. 1979, ApJ, 231, 606
Stone, E. C., et al. 1977, Space Sci. Rev., 21, 355
Webber, W. R., Kish, J. C., & Schrier, D. A. 1990a, Phys. Rev. C, 41, 520
———. 1990b, Phys. Rev. C, 41, 533
———. 1990c, Phys. Rev. C, 41, 547
Webber, W. R., Lukasiak, A., McDonald, F. B., & Ferrando, P. 1996, ApJ, 457, 435
Webber, W. R., Soutoul, A., Ferrando, P., & Gupta, M. 1990d, ApJ, 348, 611
Wiedenback, M. E., & Greiner, D. E. 1981, ApJ, 247, L122
Woosley, S. E., & Weaver, T. A. 1981, ApJ, 243, 561